Evaluation of the Sentinel-1 SAR image processing algorithms performance

Gregoriy Kaplan

GrigoriiKaplan@Gmail.com

Evaluation of the Sentinel-1 SAR image processing algorithms performance

Gregoriy Kaplan

GrigoriiKaplan@Gmail.com

Abstract

The following paper discussed the performance of previously developed SAR algorithms applied to Sentinel-1 imagery. The outputs of algorithms were correlated to top-performing Sentinel-2 reNDVI algorithms. The study found that Levelled and Normalized Sigma nought outperformed the Gamma Nought, and, especially, Sigma Nought, and RVI algorithms.

1. Introduction

Synthetic Aperture Radar (SAR) technology is used in many military [1] and civil applications [2]. Earth observation satellites equipped with a C-band (around 5.6 cm wavelength) are efficiently used for a variety of subjects such as soil moisture estimation [3,4] and a plethora of subjects related to forest and agricultural monitoring [5–7] among many others. Nevertheless, it's usage is hampered by the negative effect caused by variation of incidence angles present at different times of observations [8–11]. The goal of the present article is to perform the comparison of the effectiveness of various previously developed SAR image processing algorithms, which take incidence angle into account by the comparison with other SAR image processing algorithms. The article requires that the reader has a basic understanding of SAR technology and the complications caused by different incidence angles. The further references provide a thorough information on the SAR [12–14] and the incidence angle issue [11,15,16].

2. Materials and methods
2.1. Study site.
Sentinel-1 and Sentinel-2 imagery acquired over a large filed (Fig. 1) in a northern part of Israel was used in the study. The area of a study polygon is around 82000 square meters, covered by around 1000 pixels in the aforementioned imagery. The polygon was intentionally chosen in the
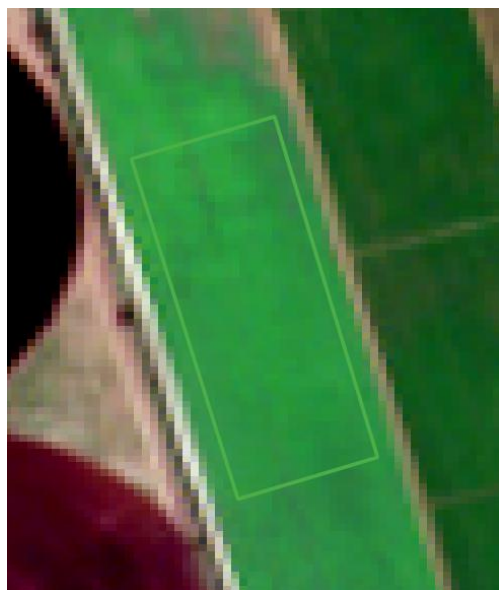
middle part of the field where vegetation was developed the most. It was done in order to avoid border effects and to develop the strongest models, which would overcome the well-known limitation of optical imager, namely saturation at the certain levels of vegetation development [17].

Fig. 1. Study site.

2.2.   Satellite imagery used in the study.

Sentinel-1 and Sentienl-2 imagery acquired between 30 May and 29 July 2023 (Fig .2).
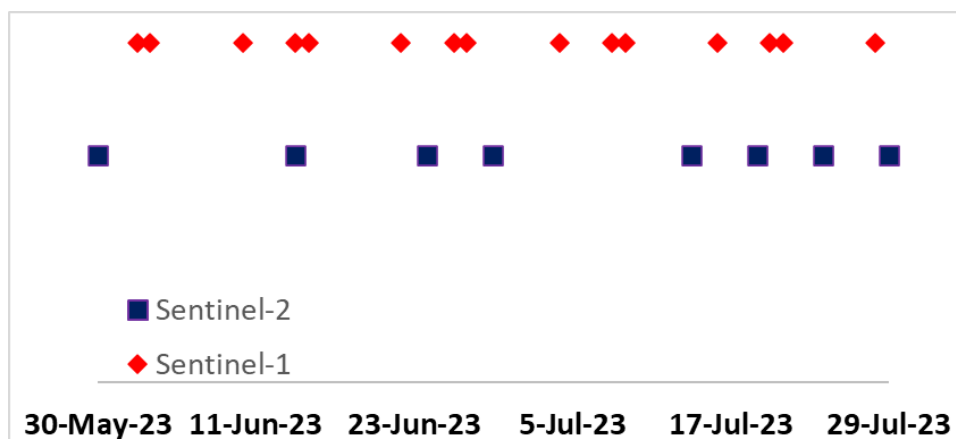
Fig. 2. Satellite imagery used in the study.

2.3.   SAR image pre-processing

Sentinel-1 SAR imagery was downloaded from Alaska Satellite Facility (https://asf.alaska.edu/datasets/daac/sentinel-1/).
Sentinel-1 SAR imagery was processed using ESA SNAP 9.0 in a standard way as follows [18]: subsetting a region around the target area, applying the latest orbit file to correct for the satellite path, thermal noise

removal, calibration to σ^0 and γ^0 and in a natural scale, range Doppler terrain correction using the SRTM 1Sec DEM. In line with the previous studies, it is important to note that all available imagery were acquired at all available incidence angles (in the range of 31-43 degrees) on both ascending and descending orbits [19].

2.4. Optical image processing.

Sentinel-2 in Level-2 processing level was downloaded from Sentinel Hub (https://apps.sentinel-hub.com/eo-browser).
Sentinel-2 imagery was processed as follows
reNDVI = (B8A − B6)/(B8A + B6),
where B8A is a Narrow NIR band (central wavelength around 865 nm) and B6 is a Red Edge 2 band (central wavelength around 740 nm). reNDVI was chosen over traditionally used vegetation indices such as NDVI because of significantly better performance of reNDVI in vegetation monitoring [20]. It is also known that best-performing vegetation indices are more accurate than ESA SNAP LAI biophysical processor [21].

2.5. Model development.

Several types of SAR image processing algorithms were performed and correlated with reNDVI Sentinel-2 acquired in the same date or to reNDVI values interpolated between closest date of Sentinel-2 data acquisition. The performance of the SAR image processing algorithms were measured using correlation coefficient (r) and RMSE.
The following SAR image processing algorithms were studied:

1) Sentinel-1 adaptation of Radar Vegetation Index (RVI) [22]

$$\text{RVI} = \frac{4*\sigma^0_{VH}}{\sigma^0_{VH} + \sigma^0_{VV}} \quad ;$$

2) $\sigma^0_{VH} - \sigma^0_{VV}$;

3) Normalized σ^0, which is calculated as follows [15]:

$\sigma^0_{Norm,VH} - \sigma^0_{Norm,VV}$, where

$\sigma^0_{Norm} = \sigma^0 * \theta$ (where σ^0 calculated separately in VV and VH polarization and θ is the local incidence angle)

4) Levelled σ^0 calculated as follows [23]:
L= H / sin (radians(90-θ)) [24],
where L is the slant radar pulse traveling distance
on its way through the atmosphere, H is the atmosphere

4

thickness in km (typically 20 km), θ is the incidence angle from the ellipsoid.

The levelling algorithm equation for VH and VV polarization:

$\sigma_\lambda = (\sigma^0 L^2) / 100,$

Finally, the following equation was calculated:

$\sigma_{\lambda,VH} - \sigma_{\lambda,VV}$

5) $\gamma^0{}_{,VH} - \gamma^0{}_{,VV.}$

γ^0 [25] is equivalent to a product that can be downloaded from the Sentinel Hub.

It should be noted that in algorithms 2-4 values of VV polarization were subtracted from VH values because it was found to be the best-performing algorithm by the comparison to other band math operations with polarization values.

All the models are the second order polynomials.
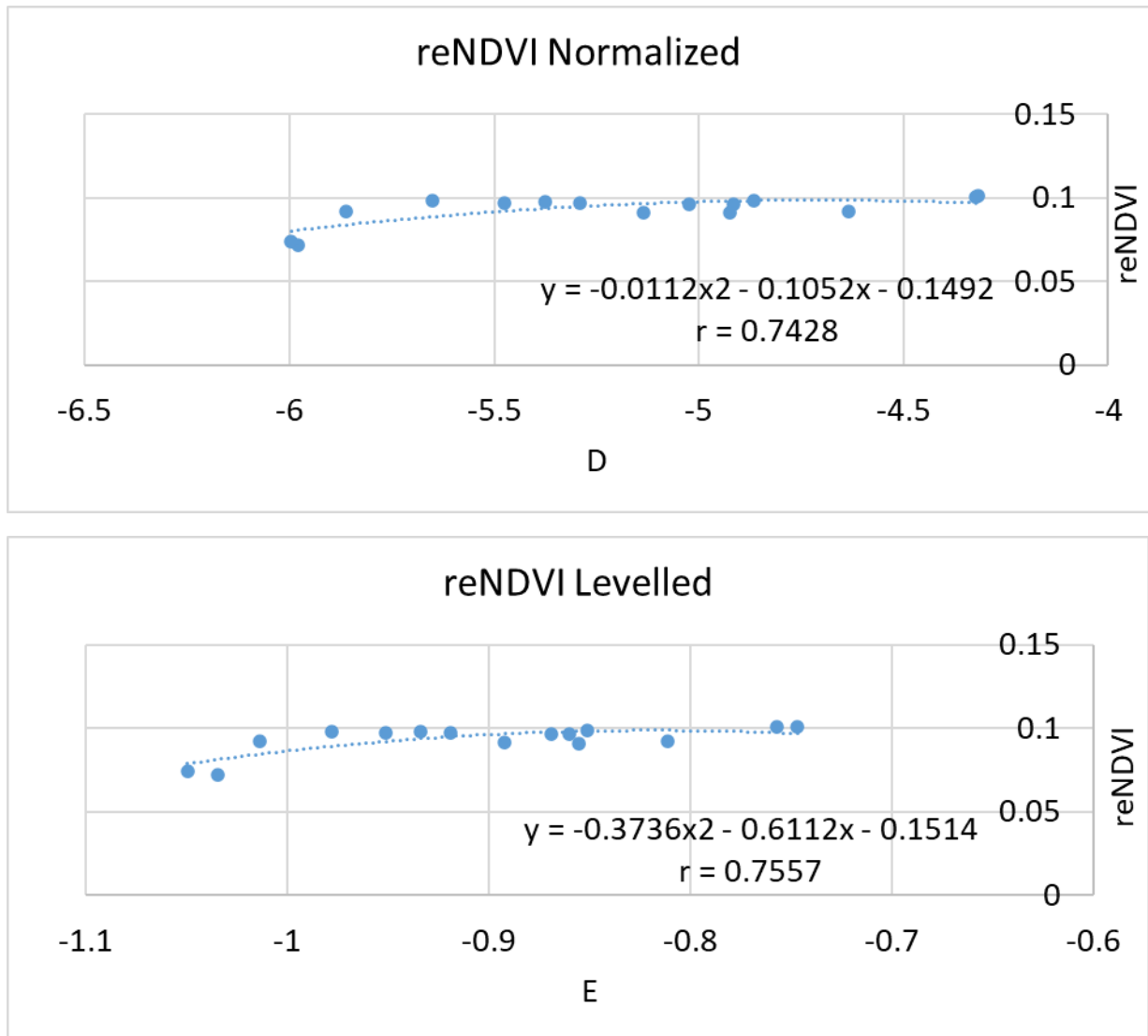
3. Results and Discussion

The following results were achieved in the study (Table 1). RVI and Sigma showed the highest RMSE and lowest r values. Gamma showed a notably better performance. The Levelled Sigma algorithm showed the best performance closely followed by Normalized Sigma.

Table 1. The performance of RVI, Sigma, Normalized Sigma and Levelled Sigma SAR algorithms cross-corelated to Sentinel-2 reNDVI. RMSE % calculated by the comparison to the best-performing Levelled Sigma SAR algorithm.

Algorithm	r	RMSE	RMSE %
RVI	0.6077	0.0067	121.2330
Sigma	0.5641	0.0070	126.0433
Gamma	0.7199	0.0059	105.9612
Normalized Sigma	0.7428	0.0058	103.8107
Levelled Sigma	0.7557	0.0056	100.0000

Fig. 2. Shows the cross-correlation equations between considered SAR algorithms and reNDVI.

reNDVI RVI

$y = -1.0066x^2 + 1.5799x - 0.5208$

$r = 0.6077$

A

reNDVI Sigma Nought

$y = -2.8351x^2 - 0.6187x + 0.0626$

$r = 0.5641$

B

reNDVI Gamma Nought

$y = -3.3156x^2 - 0.8961x + 0.0388$

$r = 0.7199$

C

Fig. 2. SAR-reNDVI cross-correlation models: A) RVI; B) Sigma Nought; C) Gamma Nought; D) Normalized Sigma Nought; E) Levelled Sigma Nought. Models B-E based on the result of the subtraction VV-polarization from VH polarization values.

Conclusion

The present study showed that Normalized and Levelled Sigma algorithms preponderate the effectiveness of other SAR image processing algorithms. As such they are recommended to use for every application of SAR imagery. Alternatively, Gamma Nought approach might be also used for a generic usage.

References

1. Reamer, R.E.; Stockton, W.O.; Stromfors, R.D. New Military Uses for Synthetic Aperture Radar (SAR). *Airborne Reconnaissance XVI* **1993**, 113–119, doi:doi:10.1117/12.140829.

2. Skolnik, M. *Radar Handbook. Third Edition*; McGraw-Hill, 2008; ISBN 978-0-07-148547-0.

3. Ettalbi, M.; Garambois, P.; Bazzi, H.; Ferreira, E. Soil Moisture Retrieval in Bare Agricultural Areas Using Sentinel-1 Images. **2023**, 1–22, doi:10.20944/preprints202306.0661.v1.

4. Singh, A.; Gaurav, K.; Meena, G.K.; Kumar, S. Estimation of Soil Moisture Applying Modified Dubois Model to Sentinel-1; A Regional Study from Central India. *Remote Sens (Basel)* **2020**, *12*, 1–19, doi:10.3390/rs12142266.

5. Löw, J.; Ullmann, T.; Conrad, C. The Impact of Phenological Developments on Interferometric and Polarimetric Crop Signatures Derived from Sentinel-1: Examples from the DEMMIN Study Site (Germany). *Remote Sens (Basel)* **2021**, *13*, 2951, doi:10.3390/rs13152951.

6. Kumar, P.; Prasad, R.; Gupta, D.K.; Mishra, V.N.; Vishwakarma, A.K.; Yadav, V.P.; Bala, R.; Choudhary, A.; Avtar, R. Estimation of Winter Wheat Crop Growth Parameters Using Time Series Sentinel-1A SAR Data. *Geocarto Int* **2018**, *33*, 942–956, doi:10.1080/10106049.2017.1316781.

7. Vadrevu, K.P. Evaluation of Sentinel-1A Data For Above Ground Biomass Estimation in Different Forests in India. **2019**.

8. David Small, Nuno Miranda, E.M. Local Incidence Angle Considered Harmful. *ACM SIGAda Ada Letters* **2009**, doi:10.1145/122028.122030.

9. Mladenova, I.E.; Jackson, T.J.; Bindlish, R.; Hensley, S. Incidence Angle Normalization of Radar Backscatter Data. *IEEE Transactions on Geoscience and Remote Sensing* **2013**, *51*, 1791–1804, doi:10.1109/TGRS.2012.2205264.

10. Topouzelis, K.; Singha, S.; Kitsiou, D. Incidence Angle Normalization of Wide Swath SAR Data for Oceanographic Applications. *Open Geosciences* **2016**, *8*, 450–464, doi:10.1515/geo-2016-0029.

11. O'Grady, D.; Leblanc, M.; Gillieson, D. Relationship of Local Incidence Angle with Satellite Radar Backscatter for Different Surface Conditions. *International Journal of Applied Earth Observation and Geoinformation* **2013**, *24*, 42–53, doi:10.1016/j.jag.2013.02.005.

12. Richards, J.A. *Remote Sensing with Imaging Radar*; Signals and Communication Technology; Springer Berlin Heidelberg: Berlin, Heidelberg, 2009; ISBN 978-3-642-02019-3.

13. Richards, J.A.; Xiuping, J. *Remote Sensing and Image Analysis*; Springer-Verlag Berlin Heidelberg, 2006; Vol. 46; ISBN 9783540251286.

14. Flores, A.; Herndon, K.; Thapa, R.; Cherrington, E. *SAR Handbook: Comprehensive Methodologies for Forest Monitoring and Biomass Estimation*; First.; SERVIR Global: Huntsville, 2019;

15. Wang, C.; Feng, M.C.; Yang, W. De; Ding, G.W.; Sun, H.; Liang, Z.Y.; Xie, Y.K.; Qiao, X.X. Impact of Spectral Saturation on Leaf Area Index and Aboveground Biomass Estimation of Winter Wheat. *Spectroscopy Letters* **2016**, *49*, 241–248, doi:10.1080/00387010.2015.1133652.

16. Kaplan, G.; Fine, L.; Lukyanov, V.; Malachy, N.; Tanny, J.; Rozenstein, O. Using Sentinel-1 and Sentinel-2 Imagery for Estimating Cotton Crop Coefficient, Height, and Leaf Area Index. *Agric Water Manag* **2023**, *276*, 108056, doi:10.1016/j.agwat.2022.108056.

17. Kaplan, G.; Gross, M.; Michel-Meyer, I.; Rahav, M.; Sela, G. DEM-Assisted in-Season Soil Moisture Estimation Based on Normalized Sentinel-1 SAR Imagery. *EarthArXiv* **2022**, 1–12, doi:https://doi.org/10.31223/X5XD0X.

18. Kaplan, G.; Rozenstein, O. Spaceborne Estimation of Leaf Area Index in Cotton, Tomato, and Wheat Using Sentinel-2. *Land (Basel)* **2021**, *10*, 505, doi:10.3390/land10050505.

19. Kaplan, G.; Fine, L.; Lukyanov, V.; Manivasagam, V.S.; Malachy, N.; Tanny, J.; Rozenstein, O. Estimating Processing Tomato Water Consumption, Leaf Area Index, and Height Using Sentinel-2 and VENµS Imagery. *Remote Sens (Basel)* **2021**, *13*, 1046, doi:10.3390/rs13061046.

20. Kim, Y.; Jackson, T.; Bindlish, R.; Lee, H.; Hong, S. Radar Vegetation Index for Estimating the Vegetation Water Content of Rice and Soybean. *IEEE Geoscience and Remote Sensing Letters* **2012**, *9*, 564–568, doi:10.1109/LGRS.2011.2174772.

21. Kaplan, G.; Fine, L.; Lukyanov, V.; Manivasagam, V.S.; Tanny, J.; Rozenstein, O. Normalizing the Local Incidence Angle in Sentinel-1 Imagery to Improve Leaf Area Index, Vegetation Height, and Crop Coefficient Estimations. *Land (Basel)* **2021**, *10*, 680, doi:10.3390/land10070680.

22. Kaplan, G.; Gross, M.; Badakhova, G.Kh. Estimation of Cotton Field Variables Using Sentinel-1 SAR Imagery Levelling Algorithm. *The scientific heritage* **2021**, *2*, 6–9, doi:10.24412/9215-0365-2021-79-2-6-9.

23. Ippolito, L.J. *Radiowave Propagation in Satellite Communications*; Springer Netherlands: Dordrecht, 1986; ISBN 978-94-011-7029-1.

24. Small, D. Flattening Gamma: Radiometric Terrain Correction for SAR Imagery. *IEEE Transactions on Geoscience and Remote Sensing* **2011**, *49*, 3081–3093, doi:10.1109/TGRS.2011.2120616.